

CrisiSense-RAG: Crisis Sensing Multimodal Retrieval-Augmented Generation for Rapid Disaster Impact Assessment

Yiming Xiao^{a,*}, Kai Yin^b, Ali Mostafavi^{a,b}

^a*Zachry Department of Civil and Environmental Engineering, Texas A&M University*

^b*Department of Computer Science and Engineering, Texas A&M University*

Abstract

Timely and spatially resolved disaster impact assessment is essential for effective emergency response. However, automated methods typically struggle with temporal asynchrony. Real-time human reports capture peak hazard conditions while high-resolution satellite imagery is frequently acquired after peak conditions. This often reflects flood recession rather than maximum extent. Naive fusion of these misaligned streams can yield dangerous underestimates when post-event imagery overrides documented peak flooding. We present CrisiSense-RAG, which is a multimodal retrieval-augmented generation framework that reframes impact assessment as evidence synthesis over heterogeneous data sources without disaster-specific fine-tuning. The system employs hybrid dense-sparse retrieval for text sources and CLIP-based retrieval for aerial imagery. A split-pipeline architecture feeds into asynchronous fusion logic that prioritizes real-time social evidence for peak flood extent while treating imagery as persistent evidence of structural damage. Evaluated on Hurricane Harvey across 207 ZIP-code queries, the framework achieves a flood extent MAE of 10.94% to 28.40% and damage severity MAE of 16.47% to 21.65% in zero-shot settings. Prompt-level alignment proves critical for quantitative validity because metric grounding improves damage estimates by up to 4.75 percentage points. These results demonstrate a practical and deployable approach to rapid resilience intelligence under real-world data constraints.

Keywords: Multimodal Retrieval-Augmented Generation (RAG), Rapid Disaster Impact Assessment, Asynchronous Data Fusion, Foundation Models for Disaster Analytics

1. Introduction

Rapid disaster impact assessment is a time-critical prerequisite for effective emergency management. Responders must quickly determine both where a hazard is occurring (e.g., flood extent) and how severe its consequences are (e.g., structural damage) to prioritize rescues and allocate scarce resources. Yet, dominant approaches remain fundamentally constrained: manual ground surveys are slow and dangerous, while physics-based hydrodynamic models are computationally expensive and struggle to reflect fast-evolving conditions at operational tempo [1]. As climate-driven extremes increase, there is an urgent need for scalable methods capable of deriving timely impact estimates

*Corresponding author

Email addresses: yxiao@tamu.edu (Yiming Xiao), kai_yin@tamu.edu (Kai Yin), amostafavi@civil.tamu.edu (Ali Mostafavi)

from the data streams already generated during disasters [2, 3]. The past decade has brought a proliferation of potentially informative data, from satellite imagery to social media streams. However, these sources are not merely heterogeneous in format; they are asynchronous in timing. Human reports and emergency calls typically peak during the hazard (capturing rising waters), while aerial and satellite imagery is frequently collected hours or days later (capturing recession).

This temporal misalignment presents a critical challenge for existing automated assessment methods. Much of the literature relies on modality-specific modeling or “naive fusion” approaches that aggregate features into a single vector such as computer vision for flood mapping or NLP for situational awareness [4, 5]. These strategies implicitly treat each data stream as a static, contemporaneous signal. When applied to asynchronous disaster data, this creates a dangerous mismatch: post-event clear-sky imagery may statistically negate earlier high-confidence flooding reports, producing underestimates precisely when accurate situational awareness is most critical. Furthermore, conventional supervised multimodal learning remains difficult to operationalize because it depends on large, labeled, multi-event datasets that are rarely available for emerging platforms or novel disaster scenarios.

To address these limitations, we reframe impact assessment as an *evidence synthesis* problem rather than a single-modality prediction task. We propose a Multimodal Retrieval-Augmented Generation (RAG) framework that leverages pre-trained foundation models to synthesize diverse data streams without event-specific fine-tuning. Unlike traditional fusion, our architecture explicitly reconciles temporal misalignment through a split-pipeline design. We employ separate Text and Visual Analyst modules to reason about modality-specific evidence, joined by an asynchronous fusion logic that treats real-time social data as evidence for peak hazard extent, while treating post-event imagery as persistent evidence of structural damage. Crucially, we enforce metric-aligned generation, ensuring outputs conform to standardized operational definitions (e.g., average damage per building, peak inundation depth) rather than qualitative severity language.

The central objective of this study is to determine whether general-purpose foundation models can deliver spatially resolved, quantitative impact estimates in a zero-shot setting. We validate this approach using Hurricane Harvey, a well-documented event with diverse data availability and measurable ground truth. Our contributions are summarized as follows:

- We demonstrate that general-purpose pre-trained language models achieve competitive performance for disaster impact assessment without task-specific fine-tuning, enabling rapid deployment across varied scenarios.
- We propose a split-pipeline Multimodal RAG architecture that explicitly handles asynchronous data streams through temporal-aware fusion logic, preventing post-event imagery from negating real-time social evidence of peak flooding.
- We provide a rigorous evaluation on Hurricane Harvey (207 queries, Greater Houston) across three diverse model backends (Gemini 2.5 Flash, Llama 3.3 70B, Qwen 2.5 72B), showing that all models produce operationally useful predictions (10.94–28.40% Extent MAE, 16.47–21.65% Damage MAE) in zero-shot settings.
- We show that prompt-level alignment through temporal context and metric grounding is essential for reliable quantitative prediction, demonstrating that careful prompt engineering can effectively compensate for the lack of task-specific training.

2. Related Work

2.1. *Remote Sensing and Automated Damage Assessment*

Satellite imagery is the standard for large-scale disaster monitoring. Recent research has focused on Deep Learning (DL) models to automate the extraction of damage features and post-event change signals at scale. Kaur et al. [6] introduced hierarchical transformers (DAHiTrA) for building localization and graded damage classification in large benchmark settings, highlighting the effectiveness of multi-resolution representations for post-disaster mapping. Similarly, Żarski and Miszczak [7] proposed multi-step feature fusion networks to improve change detection between pre- and post-event imagery, reducing missed detections when changes are subtle. To address the limitations of binary or ordinal severity scales, Xiao and Mostafavi [8] introduced DamageCAT, a typology-based framework that classifies damage into actionable categories (partial roof damage, total collapse, etc.) using hierarchical transformers on satellite image triplets, demonstrating improved transferability across multiple hurricane events. In a different direction, Pandey et al. [9] demonstrated the utility of Synthetic Aperture Radar (SAR) for flood mapping in cloud-obsured regions, emphasizing the operational value of all-weather sensing during active storm systems. For building-level flood damage, Ho and Mostafavi [10] proposed a risk-aware multimodal architecture that fuses SAR/InSAR with optical basemaps to jointly estimate floodwater extent and graded damage states, explicitly targeting cases where flood damage is nonstructural and difficult to observe in imagery alone. More recently, Ho et al. [11] integrated street-view imagery with vision-language models to estimate building elevations, illustrating how street-level visual context can complement overhead sensing for exposure-related attributes. Extending this street-level paradigm to post-disaster recovery, Xiao et al. [12] proposed Recov-Vision, a framework that links panoramic street-view video to building parcels using vision-language models to assess occupancy and habitability, capturing facade-level cues (entry blockage, temporary coverings) that overhead imagery cannot observe. However, these remote sensing methods remain limited by satellite revisit times (latency) and viewing angles, often struggling to capture lateral damage or interior flooding without corroborating ground-level evidence.

2.2. *Social Sensing: Opportunities and Uncertainties*

Social media has emerged as a critical source of real-time disaster intelligence, providing a “human sensor” network that complements remote sensing through rapid, ground-level observations. Acikara et al. [13] reviewed the field, organizing common social-analytics tasks around location awareness and situation awareness, and noting persistent challenges in noise, bias, and verification; more broadly, Zhang et al. [14] surveyed how social media supports public information and warning, peer-to-peer help, and agency listening during disasters. Specific applications include real-time sentiment analysis for flood impact [1], where online discourse is used as a proxy signal for evolving impacts, and multimodal classification of disaster losses [15], which targets fine-grained loss categories and severity cues from mixed text-image posts. Departing from conventional classifiers, instruction fine-tuning has been explored to adapt general-purpose LLMs for disaster-specific, multi-label tweet classification [16], enabling one model to extract multiple actionable labels from a single post. Zhang et al. [17] developed the SocialDISC framework to sense downstream societal impacts (e.g., power outages, road closures) from Twitter, illustrating how social streams can be transformed into structured operational indicators.

However, reliability remains a major bottleneck. Mandal et al. [18] conducted a critical study on geolocation uncertainty, finding that less than 1% of tweets are geotagged and that user profile locations have significant error margins, which can confound place-based analysis. In addition to location, the credibility of user-generated content is a persistent challenge, with noise, rumors, and hyperboles necessitating robust verification strategies. Sathianarayanan et al. [19] attempted to mitigate location uncertainty by extracting visual cues (like phone numbers) from images, offering an alternative pathway to recover location when metadata is missing. Our work addresses these dual challenges of location and credibility by using RAG to retrieve semantically relevant reports and cross-referencing them with physical imagery.

2.3. *Multimodal Data Fusion and Resilience Frameworks*

The integration of heterogeneous data is essential for Smart Resilience, typically framed through the lens of hazard, exposure, and vulnerability, and operationalized via multi-source sensing and analytics. Fan et al. [20] articulated a complementary vision of “Disaster City Digital Twins” that integrate artificial and human intelligence across heterogeneous data streams for situation assessment, decision support, and stakeholder coordination. Building on this vision, Li et al. [21] proposed Disaster Copilot, a multi-agent AI architecture where specialized sub-agents coordinate through a central orchestrator to unify predictive analytics, situational awareness, and impact assessment into a real-time operational picture, addressing the fragmented data streams and siloed technologies that hinder current practices. Yuan et al. [4] proposed a framework fusing community-scale big data (traffic, social, credit card transactions) to monitor predictive flood risk, demonstrating how diverse proxy signals can track community-level disruption. Dong et al. [5] combined channel sensor data with deep learning for hybrid flood warning systems, illustrating how learned models can complement physical sensing for early warning. Liu et al. [22] introduced FloodDamageCast, a machine learning framework for nowcasting property damage using built-environment features and data augmentation, underscoring progress toward timely consequence estimation beyond inundation mapping. While effective, these systems typically use early fusion (concatenating features) or separate model ensembles. They lack the semantic reasoning capabilities of Generative AI, which allows for the flexible interpretation of conflicting evidence (e.g., “sensor says dry” vs. “human says help”) that is characteristic of complex, asynchronous disaster scenarios.

2.4. *Multimodal Retrieval-Augmented Generation (RAG)*

RAG has reshaped how LLMs incorporate external knowledge at inference time, reducing hallucinations and improving grounding when model weights alone are insufficient [23, 24]. The extension to multimodal RAG broadens this paradigm by enabling retrieval and reasoning over both text and images within a unified evidence pipeline. Chen et al. [25] pioneered this direction with MuRAG, which couples a transformer with non-parametric multimodal memory to retrieve and condition generation on relevant visual-text evidence. Recent surveys [26] document the rapid growth of this field, including design patterns for retrieval, indexing, and multimodal fusion in generation. In domain-specific applications, RAG has shown promise in healthcare [27, 28], where grounded generation is critical for safety and traceability, and in visual document understanding [29], where retrieval helps connect layouts, text, and images to structured outputs. In the geospatial domain, Chen et al. [30] demonstrated Geospatial Awareness Layers for LLM agents in wildfire response, highlighting how spatial context can improve tool-using reasoning, and Yin et al. [31] introduced DisastIR, a benchmark that formalizes disaster information retrieval challenges for

evaluation. Our work aligns with this emerging wave of Geospatial RAG by focusing on disaster-specific constraints, especially temporally asynchronous evidence, and by emphasizing auditable, metric-aligned outputs for operational use.

3. Methodology

We present a multimodal RAG system designed to estimate flood extent and structural damage from heterogeneous, asynchronous data streams. Figure 1 illustrates our architecture, which integrates aerial imagery, social media posts, 311 emergency calls, and precipitation sensor data through a retrieval-augmented generation pipeline. The key design principle is a split-pipeline approach that processes text and visual modalities separately before fusion, respecting their distinct temporal characteristics.

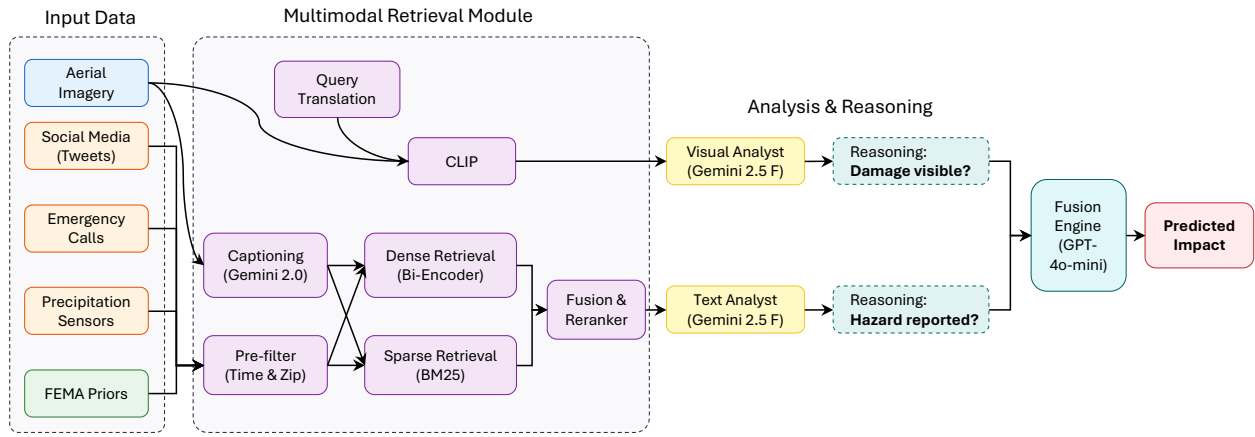


Figure 1: Overview of the proposed architecture. Our system ingests multimodal data (aerial imagery, social media, 311 calls, sensors), retrieves relevant context, and employs a split-pipeline approach with separate text and visual analyzers before fusing results.

3.1. Task Definition

We define the impact assessment task as estimating the peak flood extent and structural damage that occurred during the event (August 25–September 1, 2017), regardless of whether the water has receded at the time of retrieval. This formulation aligns with the operational needs of recovery agencies, who require a record of maximum impact rather than a transient snapshot of current conditions. Consequently, our system is designed to prioritize evidence of peak inundation (e.g., real-time social reports) over post-event evidence of recession (e.g., clear aerial imagery), unless permanent structural damage is visible.

3.2. Data Sources and Preprocessing

Our system integrates four primary data sources collected during the event, each providing complementary perspectives on disaster impact.

Aerial Imagery. We utilize high-resolution aerial imagery obtained from NOAA’s Emergency Response Imagery program [32]. The dataset comprises 3,507 georeferenced tiles covering the Greater Houston metropolitan area at 0.5m spatial resolution. Each tile is indexed by geographic coordinates and acquisition timestamp to enable spatiotemporal queries.

Visual-Text Bridging. To facilitate semantic retrieval over visual data, we employed Gemini 2.0 Flash [33] to generate natural language descriptions for all 3,507 aerial image tiles. These machine-generated captions are indexed as searchable text documents, enabling the retrieval system to surface relevant imagery based on textual queries describing observable damage patterns (e.g., submerged residential structures, debris accumulation).

FEMA Prior Knowledge. To provide historical context, we retrieve aggregated historical financial loss records from FEMA’s Individual Assistance database (2010–2016). This includes the average verified loss amount for the ZIP code from prior declared disasters. Crucially, this data represents historical vulnerability profiles established years before Hurricane Harvey and is strictly disjoint from the 2017 event-specific ground truth (depth grids and damage estimates) used for evaluation, ensuring no data leakage.

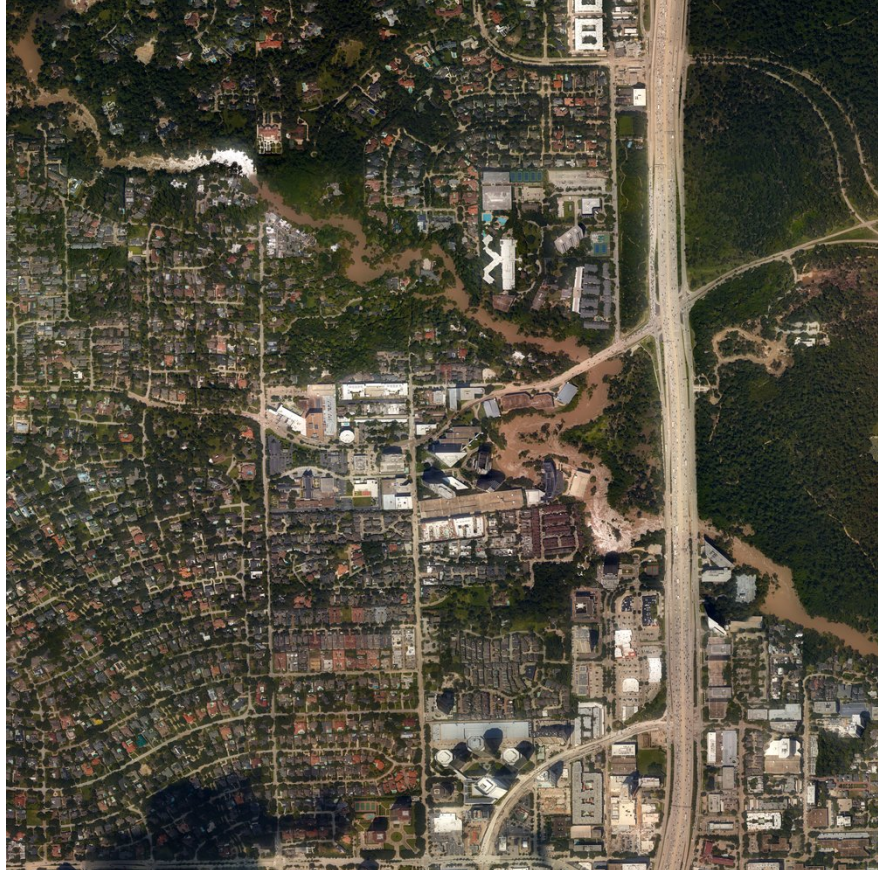


Figure 2: Example of a retrieved aerial imagery tile (Aug 31, 2017) and its machine-generated caption. The caption successfully identifies key features: *“Significant flooding is visible, with brown water inundating areas along a winding waterway... and encroaching on the highway in several places.”*

Social Media (Twitter/X). We curated a corpus from approximately 24 million tweets collected during Hurricane Harvey, applying a multi-stage filtering pipeline to maximize relevance. First, we performed de-duplication by removing retweets, which consist of approximately 57% of the raw data. Second, we applied content filtering using keyword-based allow and block lists: the allow list keeps tweets containing disaster-relevant terms (e.g., “flood,” “rescue”), while the block list excluded off-topic content (e.g., “spotify,” “music”). Third, we implemented spam removal to filter

posts containing excessive hashtags or URLs. This pipeline yielded a final corpus of 458,453 unique tweets, representing an acceptance rate of approximately 1.9%.

311 Emergency Calls. We obtain records from the City of Houston’s 311 service system, including reports of flooding, debris, and infrastructure damage. The dataset contains 26,107 records from August 20–September 10, 2017, covering 125 unique ZIP codes in the urban Houston area.

Precipitation Sensors. We incorporate data from Harris County Flood Control District rain gauges. To provide localized context, we map each target ZIP code to the nearest available sensor using a centroid-based nearest neighbor lookup, retrieving hourly precipitation measurements for the relevant time window.

3.3. Multimodal Retrieval

Given a query specifying a ZIP code and time window, our retrieval system identifies the most relevant context from each data source. The retrieval strategy differs by modality: text sources use hybrid dense-sparse retrieval with cross-encoder reranking, while visual retrieval leverages CLIP embeddings for cross-modal matching.

Text Retrieval. We employ a hybrid retrieval strategy that combines dense and sparse methods. For dense retrieval, we generate 384-dimensional text embeddings using all-MiniLM-L6-v2, selected for its efficient inference and strong performance on the MTEB benchmark [34]. Embeddings are indexed with FAISS for efficient similarity search. This is complemented by BM25-based sparse retrieval for exact keyword matching. The two retrieval methods are fused using Reciprocal Rank Fusion (RRF) with constant $k = 60$. To further refine retrieval quality, we apply a cross-encoder reranker (BAAI/bge-reranker-base), which was chosen for its ability to capture fine-grained query-document relevance and its top-tier performance on the MTEB leaderboard [35]. This reranker processes the top 20 candidates from the hybrid search.

Visual Retrieval. Complementing the text-based caption search, we employ CLIP (ViT-B/32) [36] for direct visual-semantic retrieval. This allows the system to map text queries to relevant visual features in the embedding space, retrieving imagery based on semantic content (e.g., “flooded intersection”) rather than just metadata. searches first attempt to find tiles strictly within the target ZIP code polygon. If insufficient imagery is found, the system falls back to a spatial radius search (e.g., 5km) to retrieve relevant nearby tiles from the same acquisition period.

Handling Geolocation Uncertainty. A critical challenge in social sensing is the scarcity and unreliability of precise geotags [18]. To address this, our system moves beyond coordinate-based filtering. Instead, we rely on semantic retrieval to identify tweets that are contextually relevant to the target ZIP code, even if they lack explicit GPS metadata. By retrieving posts that mention specific street names, landmarks, or neighborhoods (e.g., retrieving reports of “rescues in Bellaire” or “flooding on I-610” for relevant ZIPs despite missing GPS tags), we maximize the recall of valid on-the-ground reports without being constrained by the <1% of tweets that carry geotags. This approach inherently handles location uncertainty by prioritizing textual relevance over coordinate precision.

3.4. Split-Pipeline Architecture

A key design decision in our framework is the separation of text and visual reasoning into distinct analysis pipelines (see Figure 1). This split architecture acknowledges that text and imagery

capture fundamentally different aspects of disaster impact: text reports describe transient, real-time conditions (rising waters, rescue needs), while imagery captures persistent physical evidence (structural damage, debris). Processing them separately enables modality-specific reasoning before fusion.

Text Analyst. The Text Analyst module processes retrieved text snippets, including tweets, 311 calls, and precipitation sensor readings, and generates a structured analysis, which is the primary evidence source for local impact. We evaluate three different pre-trained language models in this role: Gemini 2.5 Flash [33], Llama 3.3 70B [37], and Qwen 2.5 72B [38].

Visual Analyst. The Visual Analyst module processes retrieved aerial imagery tiles to produce a comprehensive visual assessment of flood extent and structural damage. For Gemini experiments, we use Gemini 2.5 Flash for visual analysis; for Llama and Qwen experiments, we use GPT-4o [39] to ensure consistent visual processing capabilities across different text model backends.

Heuristic-Based Fusion Engine. We employ a heuristic-based fusion strategy that combines estimates from the Text and Visual Analysts based on the temporal characteristics of the evidence. As formally defined below, this module mitigates the “snapshot vs. peak” problem by prioritizing text for flood extent (to capture receding waters) while treating visual evidence as additive for structural damage.

To formally define the integration of asynchronous modalities, we employ a heuristic fusion logic that respects the temporal characteristics of each stream:

Algorithm 1 Asynchronous Multimodal Fusion Logic

Input: Text Analysis (T), Visual Analysis (V), Query Date (D_Q), Peak Date (D_P)
Output: Flood Extent (E), Damage Severity (S)

```

// 1. Hazard (Flood Extent): Prioritize real-time text
if  $D_Q > D_P$  AND  $V$  shows “Recession” then
     $E \leftarrow T_{extent}$  {Ignore clear post-event imagery}
else
     $E \leftarrow \text{WeightedAvg}(T_{extent}, V_{extent})$ 
end if

// 2. Consequence (Damage): Additive evidence
// Visual damage (debris) is persistent; Text damage (interiors) is hidden
 $S \leftarrow \max(T_{damage}, V_{damage})$ 
return  $E, S$ 

```

As shown in Algorithm 1, this logic ensures that a clear post-event image does not veto a high-confidence text report of earlier flooding (preventing false negatives in extent), while ensuring that visible structural debris in imagery contributes to the damage score even if text reports are sparse (preventing false negatives in damage).

3.5. Reasoning and Alignment Strategy

A core challenge in multimodal disaster assessment is the temporal mismatch between real-time text reports and post-event data. We address this through explicit reasoning instructions:

- **Temporal Context:** Text sources typically report conditions during peak flooding (e.g., August 27–28), while precipitation sensors and imagery are often captured post-event (September). To prevent the model from misinterpreting the end of rainfall as a lack of flooding, we instruct the system that sensor data showing “0.0 inches” during post-event periods indicates “storm has passed and water is likely receding,” not “no flooding occurred.” Consequently, the system prioritizes concurrent text reports for flood extent assessment.
- **Metric-Aligned Reasoning:** A critical failure mode in standard RAG is metric misalignment, where LLMs interpret “damage severity” as a qualitative intensity score (e.g., “catastrophic” = 90%) rather than the specific statistical definition of the ground truth. We introduce a Metric Alignment Constraint in the system prompt that explicitly defines `damage_severity_pct` as the average damage ratio across all structures in the ZIP code (0–100%). This forces the model to perform an implicit denominator estimation (e.g., “reports show 50 flooded homes in a neighborhood of around 500, implying about 10% severity”) rather than reacting solely to the emotional intensity of individual reports. As shown in our ablation study (Section 5.1), this single intervention reduces error by 4.75 percentage points, demonstrating that domain-specific statistical grounding is as critical as retrieval quality.

4. Experiments and Results

4.1. Dataset

We evaluate CrisiSense-RAG on data from Hurricane Harvey, which made landfall on August 25, 2017, causing unprecedented flooding in the Greater Houston area. Harvey stalled over the region for four days, dropping over 60 inches of rain in some areas and affecting over 300,000 structures. Table 1 summarizes our data sources.

Table 1: Dataset statistics for the Hurricane Harvey evaluation.

| Data Source | Count | Coverage |
|---------------------------------|------------------|-----------------|
| Aerial Imagery Tiles | 3,507 | Greater Houston |
| Image Captions | 3,507 | Greater Houston |
| Tweets (filtered) | 458,453 | Harris County |
| 311 Emergency Calls | 26,107 | City of Houston |
| Precipitation Sensors | 15 (330 records) | Harris County |
| Property Damage Extent | 72,755 | 139 ZIPs |
| Queries | 207 | Study Area |
| Flood Depth Grid (ground truth) | 33,144 ZIPs | Texas-wide |

We employ a dual ground-truth framework to evaluate the distinct Hazard and Consequence outputs of CrisiSense-RAG:

- **Hazard Ground Truth (Flood Extent):** We use the FEMA Harvey Flood Depth Grid [40] to compute the percentage of each ZIP code covered by water (`flooded_pct`). This is the target for the model’s `flood_extent_pct` prediction.

- **Damage Ground Truth (Structural Severity):** We utilize Property Damage Extent (PDE) proposed and computed by Ma et al. [41] from 139 ZIP codes to quantify structural impact. The ground truth is $\text{mean_pde} \times 100$, where mean_pde represents the average damage per building across all buildings in a ZIP code (0–1 range). This is the target for the model’s `damage_severity_pct` prediction, which we explicitly define as “average damage per building” to ensure semantic alignment. PDE coverage does not span the full 207 ZIPs, so 68 ZIPs lack damage ground truth and are treated as missing in the spatial maps.

We construct evaluation queries with a stratified sampling design to ensure diverse geographic and data coverage. Our main results are reported on the full study area of 207 queries, covering 207 unique ZIP codes in the Greater Houston region. This expanded evaluation set includes both high-activity urban ZIP codes and suburban/peripheral areas, providing a comprehensive assessment of system scalability and generalization. All queries target the primary Hurricane Harvey impact window (August 25–September 1, 2017), capturing the full progression from landfall through the peak flooding period.

4.2. Ablation Study Design

We conduct a systematic ablation study to quantify the contribution of each modality and reasoning strategy. By progressively adding components (captions, direct visual analysis) to a text-only baseline, we isolate the value of each modality for flood extent versus damage severity prediction. Note that we do not compare against supervised baselines (e.g., DAHiTrA [6] or FloodDamageCast [22]) as our goal is to evaluate the zero-shot capabilities of general-purpose models, not to compete with task-specific models trained on historical data. Consequently, our comparison focuses on internal ablations.

- **Text-Only RAG:** Baseline RAG using only text sources (tweets, 311 calls, sensors) without any imagery input. This represents a purely text-based assessment approach.
- **Text and Caption RAG:** RAG with text sources augmented by image captions. Captions are generated from aerial imagery using Gemini 2.0 Flash and indexed as searchable text. This tests whether semantic descriptions of imagery can bridge the modality gap without direct visual analysis.
- **Full Multimodal RAG:** Complete split-pipeline architecture with separate Text Analyst and Visual Analyst modules. The Visual Analyst directly processes aerial imagery tiles (using Gemini 2.5 Flash for Gemini experiments, GPT-4o for Llama/Qwen experiments), providing independent visual assessment that is fused with text analysis using heuristic rules. Table 2 summarizes the experimental configurations.

Prompt Strategies. As described in Section 3.5, we compare standard prompting against our optimized strategy which includes explicit temporal context (interpreting post-event sensor data correctly) and semantic alignment (defining damage severity as per-building average). These strategies are ablated to measure their specific impact on system performance.

Table 2: Model configurations and visual backends. Llama and Qwen use GPT-4o for visual tasks, while Gemini relies on its native multimodal capability. Text-only setups have no visual backend; all image captions were generated with Gemini 2.0 Flash.

| Foundation Text Model | Caption Provider | Visual Analyst |
|-----------------------|------------------|------------------|
| Gemini 2.5 Flash | | Gemini 2.5 Flash |
| Llama 3.3 70B | Gemini 2.0 Flash | GPT-4o |
| Qwen 2.5 72B | | GPT-4o |

4.3. Evaluation Metrics

We evaluate prediction accuracy using Mean Absolute Error (MAE) for both Hazard (Flood Extent) and Consequence (Damage Severity). MAE measures the average absolute deviation between predicted percentages (0–100%) and ground truth values. We report separate MAE scores for flood extent (`flooded_pct`) and damage severity ($\text{mean_pde} \times 100$), allowing us to assess performance on each distinct output of our dual-metric system.

4.4. Main Results

Table 3 and Figure 3 show the main quantitative results from our ablation study, which compares three configurations: text-only, text with captions, and full multimodal RAG. We report Mean Absolute Error (MAE) separately for flood extent and damage severity, as these metrics target distinct ground truth sources and exhibit different modality dependencies.

Table 3: Main results on the full study area ($N = 207$). We report Mean Absolute Error (MAE) with bootstrapped 95% confidence intervals. All models operate in a zero-shot setting. Lower values indicate better performance.

| Model & Configuration | Extent MAE (95% CI) | Damage MAE (95% CI) |
|-------------------------|-----------------------------|-----------------------------|
| <i>Gemini 2.5 Flash</i> | | |
| Text-Only | 28.40 [25.65, 31.15] | 18.66 [16.63, 20.70] |
| Text+Caption | 28.35 [25.79, 30.92] | 17.78 [15.78, 19.78] |
| Multimodal | 26.98 [24.38, 29.57] | 18.20 [16.31, 20.10] |
| <i>Llama 3.3 70B</i> | | |
| Text-Only | 10.94 [9.58, 12.30] | 16.47 [15.24, 17.69] |
| Text+Caption | 10.94 [9.61, 12.26] | 16.60 [15.39, 17.80] |
| Multimodal | 11.11 [9.68, 12.53] | 16.71 [15.22, 18.20] |
| <i>Qwen 2.5 72B</i> | | |
| Text-Only | 16.79 [15.23, 18.35] | 20.80 [18.81, 22.78] |
| Text+Caption | 18.09 [16.49, 19.69] | 21.65 [19.69, 23.62] |
| Multimodal | 22.70 [21.07, 24.34] | 21.56 [19.52, 23.61] |

General-purpose pre-trained models demonstrated consistent capability across diverse configurations. For Gemini 2.5 Flash, the Text+Caption configuration yielded the most accurate damage assessments (17.78% MAE), supporting the hypothesis that semantic descriptions can effectively bridge the modality gap. The split-pipeline architecture proved particularly robust; by largely

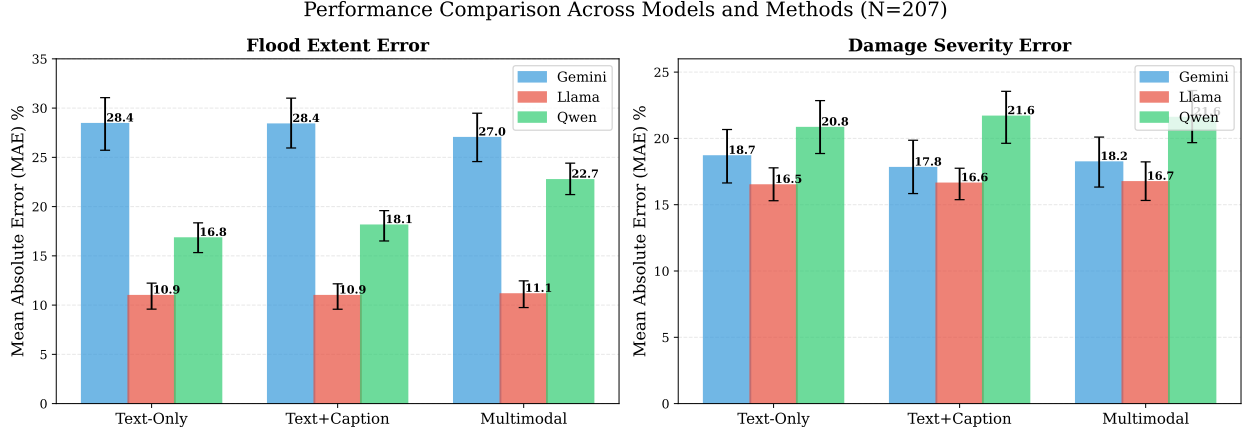


Figure 3: Performance comparison across methods and models on the full study area ($N = 207$). Each panel shows results for one model (Gemini 2.5 Flash, Llama 3.3 70B, Qwen 2.5 72B) across three configurations: Text-Only, Text+Caption, and Multimodal. Performance patterns vary by model and configuration, with Llama showing the lowest errors overall and Qwen showing stronger performance in text-only settings (see Table 3 for detailed statistics).

isolating the flood extent prediction to social text signals, the system avoided the common pitfall of underestimation caused by post-event “clear” imagery. However, as noted in the prompt engineering ablation (Section 3.5), this architectural benefit is contingent on explicit temporal reasoning instructions.

To validate that our approach works with diverse pre-trained models without task-specific fine-tuning, we evaluated the split-pipeline design with three distinct text models: Gemini 2.5 Flash (closed-source), Llama 3.3 70B, and Qwen 2.5 72B (open-source). Table 3 and Figure 3 reveal that all three models achieve reasonable performance in zero-shot settings, with Extent MAE ranging from 10.94% (Llama Text-Only) to 28.40% (Gemini Text-Only) and Damage MAE ranging from 16.47% (Llama Text-Only) to 21.65% (Qwen Text+Caption). While performance varies by model and configuration, all models produce operationally useful predictions without any disaster-specific training, demonstrating the practical viability of deploying pre-trained models for disaster impact assessment.

Notably, the best-performing configuration varies by model: for Gemini, Text+Caption achieves the best damage assessment (17.78% MAE); for Llama, Text-Only performs best on both metrics (10.94% Extent, 16.47% Damage); for Qwen, Text-Only performs best (16.79% Extent, 20.80% Damage). This variation suggests that different pre-trained models have different strengths, and the optimal configuration depends on the specific model and use case. However, the key finding is that all models achieve reasonable performance across configurations, confirming that general-purpose pre-trained models can be effectively deployed for disaster assessment without the resource-intensive requirements of collecting large task-specific datasets or training specialized models. This makes our approach promising for widespread adoption in emergency management contexts where rapid deployment and ease of implementation are critical.

4.5. Spatial Distribution of Impact

Figure 4 illustrates the spatial alignment between ground truth and model predictions for both flood extent and damage severity across the core 139 ZIP codes. Visually, the model effectively captures the broad geographic distribution of flooding, accurately identifying high-impact areas

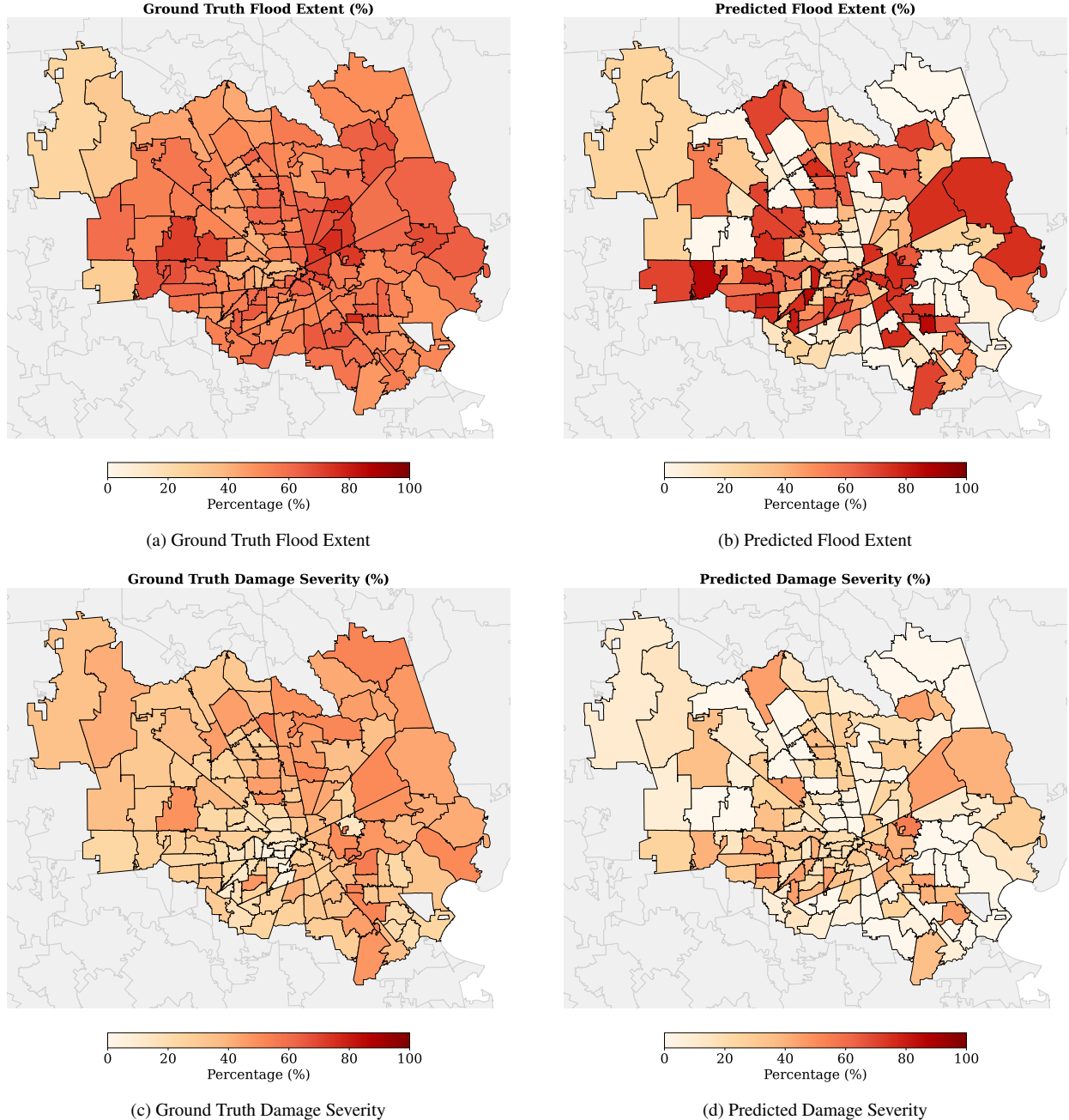


Figure 4: Spatial comparison of Ground Truth vs. CrisiSense-RAG predictions for Flood Extent (Top) and Damage Severity (Bottom). Only areas with PDE data are shown here. The model successfully captures the broad spatial distribution of flooding and the specific pockets of severe structural damage across the Greater Houston area.

along major waterways and reservoirs. For damage severity, the predictions show strong spatial agreement with the clusters of structural damage recorded in the Property Damage Extent (PDE). Notably, by focusing the visualization and evaluation on the core area where ground truth coverage is most complete, we observe that the system successfully disambiguates localized hazard reports into a coherent geographic assessment. While the model occasionally over-predicts or under-predicts impact in areas with dense social media activity, the overall spatial correspondence validates our approach’s utility for rapid situational awareness.

5. Analysis

5.1. Ablation Study

We conduct ablation experiments to isolate the contribution of prompt-level interventions. Table 4 quantifies the impact of semantic alignment and temporal context instructions, both of which proved essential for achieving reliable predictions.

Table 4: Prompt engineering ablation study. We measure the impact of key prompt improvements on prediction accuracy.

| Prompt Improvement | Target Metric | Δ MAE (pp) |
|-------------------------------------------------------|-----------------|-------------------|
| Semantic Alignment (“average damage per building”) | Damage Severity | –4.75 |
| Temporal Context (sensor data interpretation) | Flood Extent | –1.65 |
| Combined Effect | Both | Best overall |

5.1.1. Impact of Reasoning Strategies

Table 4 quantifies the impact of the prompt-based interventions described in Section 3.5. Our results demonstrate that domain-specific alignment is a critical factor in zero-shot performance: enforcing statistical definitions and temporal context yields performance gains comparable to, or exceeding, those achieved by model scaling.

Semantic Alignment: This intervention, which defines damage severity as a statistical average (see Section 3.5), improved damage MAE by 4.75 percentage points. It effectively corrected a systematic bias where the model overestimated damage based on broad qualitative descriptors like “widespread.”

Temporal Context: Clarifying post-event sensor data improved flood extent prediction by 1.65 percentage points, particularly in the post-peak window (Sept 1–10) where dry sensors were previously misinterpreted as an absence of historical flooding. Crucially, this context also prevents the asynchronous fusion failure mode where post-event “clear” imagery would mistakenly negate high-confidence text reports of peak flooding. By prioritizing real-time evidence for hazard extent, this strategy resolves conflict between asynchronous signals and prevents systematic underestimation.

5.1.2. Retrieval Quality

We validated the retrieval pipeline by analyzing the content of all retrieved tweets ($N = 4,140$) across the 207 queries. On average, the system retrieved 20.0 tweets per query. Topic relevance was near-perfect (99.7% contained disaster keywords), and despite the scarcity of geotags, 60.0% of retrieved tweets contained explicit geographic mentions (e.g., street names, neighborhoods), confirming the effectiveness of semantic search in grounding evidence.

5.2. Error Analysis

We present two representative failure cases that illustrate the primary error modes of our system.

Failure Case 1: Underestimation (ZIP 77061). Ground Truth: 57.3% | Prediction: 0.5% | **Abs. Error: 56.8 pp**

Retrieved Evidence: Tweets (20): “It’s not flooded in my zip code 77061 and we have been without power since Saturday” (902310479695147013); “Historic flooding in Houston area” (901826476210876417); “Hurricane Harvey damage” (901849278003372034). Sensor: 0.0 inches (Sept 10, post-event). 311 Calls: None retrieved. Imagery: 6 tiles retrieved; visual analysis unavailable.

Model Reasoning: “The primary evidence for ZIP 77061 is Tweet ID [902310479695147013], which explicitly states ‘It’s not flooded in my zip code 77061’. This direct, on-the-ground report strongly indicates that widespread flooding did not occur in this specific ZIP code. There are no other tweets or 311 calls that contradict this statement.”

Failure Mode: A single contrarian tweet dominated reasoning, overriding regional evidence of historic flooding. The model over-weighted one resident’s hyper-local observation (their immediate surroundings) as representative of the entire ZIP code, which spans several square miles.

Failure Case 2: Overestimation (ZIP 77494). Ground Truth: 28.7% | Prediction: 75.0% | **Abs. Error: 46.3 pp**

Retrieved Evidence:

Tweets (20): “Harvey unleashes historic flooding in Houston area” (901826476210876417); “1,000-year flood event unprecedented in scale” (903399005224357889); “no words for the amount of flood damage I’ve seen up close in Bellaire” (903028781920788480); “Hurricane Harvey destroyed a lot” (903081533124247553). Sensor: 0.0 inches (Sept 10, post-event). 311 Calls: None retrieved. Imagery: 6 tiles; visual analysis showed no active flooding (conflict resolved by trusting text).

Model Reasoning: “The provided tweets consistently report ‘historic flooding’ and ‘widespread damage’ across the broader Houston area. While no specific reports directly name ZIP 77494, the pervasive nature of these reports strongly indicates that a ZIP code within Harris County would experience significant impact.”

Failure Mode: General Houston-area reports were extrapolated to this specific suburban ZIP code. The tweets describe regional impact but lack ZIP-specific ground-level observations. This peripheral area experienced 28.7% flooding, significant but far less than the 75% predicted from regional generalization.

Our analysis reveals three primary error categories: (1) contrarian report bias, where a single tweet claiming “no flooding” overrides aggregate evidence; (2) regional generalization, where Houston-wide reports are incorrectly extrapolated to specific ZIP codes; and (3) false positives from misinterpreting normal water features as flood damage. Qualitative success cases showing accurate regional and local inference are provided in Appendix C.

6. Conclusion

We presented CrisiSense, a multimodal retrieval-augmented generation framework for disaster impact assessment that leverages general-purpose pre-trained language models without task-specific fine-tuning. Through systematic evaluation on Hurricane Harvey data ($N = 207$ queries) across three diverse model backends (Gemini 2.5 Flash, Llama 3.3 70B, Qwen 2.5 72B), we demonstrated that pre-trained models achieve reasonable performance (Extent MAE: 10.94–28.40%, Damage MAE: 16.47–21.65%) in zero-shot settings, enabling rapid deployment across varied disaster scenarios without the resource-intensive requirements of collecting large task-specific datasets or training specialized models. For multimodal configurations, we used GPT-4o for visual analysis with Llama and Qwen text models to ensure consistent visual processing capabilities.

By demonstrating that general-purpose pre-trained models can be deployed without task-specific fine-tuning, we establish a new baseline for rapid disaster response. Our proposed split-pipeline architecture resolves the critical issue of temporal misalignment, ensuring that post-event imagery does not negate real-time social signals. Furthermore, our findings regarding prompt-level alignment confirm that careful metric grounding can effectively compensate for the lack of specialized training data, yielding substantial improvements of up to 4.75 percentage points, which confirms the crucial role of structured prompts in zero-shot reasoning.

Critically, our evaluation reveals that this split-pipeline architectural approach enables consistent, operationally useful predictions across all pre-trained models. This supports our core hypothesis: while specialized models trained on massive historical datasets may offer superior precision, pre-trained models provide an accessible and immediate capability that is sufficient for many rapid response needs. This trade-off—sacrificing some precision for massive gains in deployability—makes pre-trained RAG systems a promising path for democratizing disaster analytics.

6.1. Limitations and Future Work

Our study focuses on Hurricane Harvey (Harris County, TX), so generalizability to other disaster types and geographies remains to be verified. While semantic retrieval improves coverage, it may introduce spatial noise compared to precise coordinate filtering. Finally, the damage evaluation is constrained by the availability of ground truth estimates for only 139 ZIP codes.

Future work should extend the framework to multi-hazard events (wildfires, earthquakes), incorporate real-time streaming data sources, and add calibrated uncertainty estimates to help emergency managers triage predictions. Developing human-in-the-loop interfaces for expert validation would further improve both accuracy and operational trust.

6.2. Broader Impact

This framework has potential to assist emergency responders in rapid damage assessment by synthesizing heterogeneous information sources. Unlike black-box models, the retrieval-based design provides an auditable trail of evidence (e.g., source tweets, imagery), allowing analysts to verify

predictions. However, automated systems should augment rather than replace human judgment. Our error analysis reveals susceptibility to contrarian reports and regional over-generalization, which could misallocate resources if predictions are accepted uncritically. We recommend operational deployments include confidence thresholds for human review and explicit reasoning disclosure for verification. Finally, communities with lower social media penetration may be underrepresented, and future work should evaluate and mitigate such biases to ensure equitable disaster response.

Acknowledgements

The authors would like to thank Junwei Ma for providing the Property Damage Extent (PDE) dataset used as part of the ground truth in this study.

Funding

This research did not receive any specific grant from funding agencies in the public, commercial, or not-for-profit sectors.

Code and Data Availability

The code used in this study is publicly available on GitHub. The dataset is available on Hugging Face.

References

- [1] Lydia Bryan-Smith, Jake Godsall, Franky George, Kelly Egode, Nina Dethlefs, and Dan Parsons. Real-time social media sentiment analysis for rapid impact assessment of floods. *Computers & Geosciences*, 178:105405, September 2023. ISSN 00983004. doi: 10.1016/j.cageo.2023.105405. URL <https://linkinghub.elsevier.com/retrieve/pii/S0098300423001097>.
- [2] Zhewei Liu, Natalie Coleman, Flavia Ioana Patrascu, Kai Yin, Xiangpeng Li, and Ali Mostafavi. Artificial intelligence for flood risk management: A comprehensive state-of-the-art review and future directions. *International Journal of Disaster Risk Reduction*, 117:105110, February 2025. ISSN 22124209. doi: 10.1016/j.ijdrr.2024.105110. URL <https://linkinghub.elsevier.com/retrieve/pii/S2212420924008720>.
- [3] Moez Krichen, Mohamed S. Abdalzaher, Mohamed Elwekeil, and Mostafa M. Fouda. Managing natural disasters: An analysis of technological advancements, opportunities, and challenges. *Internet of Things and Cyber-Physical Systems*, 4:99–109, 2024. ISSN 26673452. doi: 10.1016/j.iotcps.2023.09.002. URL <https://linkinghub.elsevier.com/retrieve/pii/S2667345223000500>.
- [4] Faxi Yuan, Chao Fan, Hamed Farahmand, Natalie Coleman, Amir Esmalian, Cheng-Chun Lee, Flavia I Patrascu, Cheng Zhang, Shangjia Dong, and Ali Mostafavi. Smart flood resilience: harnessing community-scale big data for predictive flood risk monitoring, rapid impact assessment, and situational awareness. *Environmental Research: Infrastructure and Sustainability*, 2(2):025006, June 2022. ISSN 2634-4505. doi: 10.1088/2634-4505/ac7251. URL <https://iopscience.iop.org/article/10.1088/2634-4505/ac7251>.

[5] Shangjia Dong, Tianbo Yu, Hamed Farahmand, and Ali Mostafavi. A hybrid deep learning model for predictive flood warning and situation awareness using channel network sensors data. *Computer-Aided Civil and Infrastructure Engineering*, 36(4):402–420, April 2021. ISSN 1093-9687, 1467-8667. doi: 10.1111/mice.12629. URL <https://onlinelibrary.wiley.com/doi/10.1111/mice.12629>.

[6] Navjot Kaur, Cheng-Chun Lee, Ali Mostafavi, and Ali Mahdavi-Amiri. Large-scale building damage assessment using a novel hierarchical transformer architecture on satellite images. *Computer-Aided Civil and Infrastructure Engineering*, 38(15):2072–2091, October 2023. ISSN 1093-9687, 1467-8667. doi: 10.1111/mice.12981. URL <https://onlinelibrary.wiley.com/doi/10.1111/mice.12981>.

[7] Mateusz Żarski and Jarosław A. Miszczak. Multi-Step Feature Fusion for Natural Disaster Damage Assessment on Satellite Images. *IEEE Access*, 12:140072–140081, 2024. ISSN 2169-3536. doi: 10.1109/ACCESS.2024.3459424. URL <https://ieeexplore.ieee.org/document/10679116/>.

[8] Yiming Xiao and Ali Mostafavi. DamageCAT: A deep learning transformer framework for typology-based post-disaster building damage categorization. *International Journal of Disaster Risk Reduction*, 128:105704, October 2025. ISSN 22124209. doi: 10.1016/j.ijdrr.2025.105704. URL <https://linkinghub.elsevier.com/retrieve/pii/S221242092500528X>.

[9] Arvind Chandra Pandey, Kavita Kaushik, and Bikash Ranjan Parida. Google Earth Engine for Large-Scale Flood Mapping Using SAR Data and Impact Assessment on Agriculture and Population of Ganga-Brahmaputra Basin. *Sustainability*, 14(7):4210, April 2022. ISSN 2071-1050. doi: 10.3390/su14074210. URL <https://www.mdpi.com/2071-1050/14/7/4210>.

[10] Yu-Hsuan Ho and Ali Mostafavi. Multimodal Mamba with multitask learning for building flood damage assessment using synthetic aperture radar remote sensing imagery. *Computer-Aided Civil and Infrastructure Engineering*, 40(26):4401–4424, November 2025. ISSN 1093-9687, 1467-8667. doi: 10.1111/mice.70059. URL <https://onlinelibrary.wiley.com/doi/10.1111/mice.70059>.

[11] Yu-Hsuan Ho, Longxiang Li, and Ali Mostafavi. Integrated vision language and foundation model for automated estimation of building lowest floor elevation. *Computer-Aided Civil and Infrastructure Engineering*, 40(1):75–90, January 2025. ISSN 1093-9687, 1467-8667. doi: 10.1111/mice.13310. URL <https://onlinelibrary.wiley.com/doi/10.1111/mice.13310>.

[12] Yiming Xiao, Archit Gupta, Miguel Esparza, Yu-Hsuan Ho, Antonia Sebastian, Hannah Weas, Rose Houck, and Ali Mostafavi. Recov-vision: Linking street view imagery and vision-language models for post-disaster recovery, 2025. URL <https://arxiv.org/abs/2509.20628>.

[13] Turgut Acikara, Bo Xia, Tan Yigitcanlar, and Carol Hon. Contribution of Social Media Analytics to Disaster Response Effectiveness: A Systematic Review of the Literature. *Sustainability*, 15(11):8860, May 2023. ISSN 2071-1050. doi: 10.3390/su15118860. URL <https://www.mdpi.com/2071-1050/15/11/8860>.

- [14] Cheng Zhang, Chao Fan, Wenlin Yao, Xia Hu, and Ali Mostafavi. Social media for intelligent public information and warning in disasters: An interdisciplinary review. *International Journal of Information Management*, 49:190–207, December 2019. ISSN 02684012. doi: 10.1016/j.ijinfomgt.2019.04.004. URL <https://linkinghub.elsevier.com/retrieve/pii/S0268401218310995>.
- [15] Wei Zhou, Lu An, Ruilian Han, and Gang Li. Classification and severity assessment of disaster losses based on multi-modal information in social media. *Information Processing & Management*, 62(5):104179, September 2025. ISSN 03064573. doi: 10.1016/j.ipm.2025.104179. URL <https://linkinghub.elsevier.com/retrieve/pii/S0306457325001207>.
- [16] Kai Yin, Bo Li, Chengkai Liu, Ali Mostafavi, and Xia Hu. Crisissense-llm: Instruction fine-tuned large language model for multi-label social media text classification in disaster informatics, 2025. URL <https://arxiv.org/abs/2406.15477>.
- [17] Cheng Zhang, Wenlin Yao, Yang Yang, Ruihong Huang, and Ali Mostafavi. Semiautomated social media analytics for sensing societal impacts due to community disruptions during disasters. *Computer-Aided Civil and Infrastructure Engineering*, 35(12):1331–1348, December 2020. ISSN 1093-9687, 1467-8667. doi: 10.1111/mice.12576. URL <https://onlinelibrary.wiley.com/doi/10.1111/mice.12576>.
- [18] Debayan Mandal, Lei Zou, Joynal Abedin, Bing Zhou, Mingzheng Yang, Binbin Lin, and Heng Cai. Algorithmic uncertainties in geolocating social media data for disaster management. *Cartography and Geographic Information Science*, 51(4):565–582, July 2024. ISSN 1523-0406, 1545-0465. doi: 10.1080/15230406.2023.2286385. URL <https://www.tandfonline.com/doi/full/10.1080/15230406.2023.2286385>.
- [19] Manikandan Sathianarayanan, Pai-Hui Hsu, and Chy-Chang Chang. Extracting disaster location identification from social media images using deep learning. *International Journal of Disaster Risk Reduction*, 104:104352, April 2024. ISSN 22124209. doi: 10.1016/j.ijdrr.2024.104352. URL <https://linkinghub.elsevier.com/retrieve/pii/S2212420924001146>.
- [20] Chao Fan, Cheng Zhang, Alex Yahja, and Ali Mostafavi. Disaster City Digital Twin: A vision for integrating artificial and human intelligence for disaster management. *International Journal of Information Management*, 56:102049, February 2021. ISSN 02684012. doi: 10.1016/j.ijinfomgt.2019.102049. URL <https://linkinghub.elsevier.com/retrieve/pii/S0268401219302956>.
- [21] Bo Li, Junwei Ma, Kai Yin, Yiming Xiao, Chia-Wei Hsu, and Ali Mostafavi. Disaster management in the era of agentic ai systems: A vision for collective human-machine intelligence for augmented resilience, 2025. URL <https://arxiv.org/abs/2510.16034>.
- [22] Chia-Fu Liu, Lipai Huang, Kai Yin, Sam Brody, and Ali Mostafavi. FloodDamageCast: Building flood damage nowcasting with machine-learning and data augmentation. *International Journal of Disaster Risk Reduction*, 114:104971, November 2024. ISSN 22124209. doi: 10.1016/j.ijdrr.2024.104971. URL <https://linkinghub.elsevier.com/retrieve/pii/S2212420924007337>.

[23] Agada Joseph Oche, Ademola Glory Folashade, Tirthankar Ghosal, and Arpan Biswas. A Systematic Review of Key Retrieval-Augmented Generation (RAG) Systems: Progress, Gaps, and Future Directions, July 2025. URL <http://arxiv.org/abs/2507.18910>. arXiv:2507.18910 [cs].

[24] Xiaohua Wang, Zhenghua Wang, Xuan Gao, Feiran Zhang, Yixin Wu, Zhibo Xu, Tianyuan Shi, Zhengyuan Wang, Shizheng Li, Qi Qian, Ruicheng Yin, Changze Lv, Xiaoqing Zheng, and Xuanjing Huang. Searching for Best Practices in Retrieval-Augmented Generation. In *Proceedings of the 2024 Conference on Empirical Methods in Natural Language Processing*, pages 17716–17736, Miami, Florida, USA, 2024. Association for Computational Linguistics. doi: 10.18653/v1/2024.emnlp-main.981. URL <https://aclanthology.org/2024.emnlp-main.981>.

[25] Wenhui Chen, Hexiang Hu, Xi Chen, Pat Verga, and William Cohen. MuRAG: Multimodal Retrieval-Augmented Generator for Open Question Answering over Images and Text. In *Proceedings of the 2022 Conference on Empirical Methods in Natural Language Processing*, pages 5558–5570, Abu Dhabi, United Arab Emirates, 2022. Association for Computational Linguistics. doi: 10.18653/v1/2022.emnlp-main.375. URL <https://aclanthology.org/2022.emnlp-main.375>.

[26] Mohammad Mahdi Abootorabi, Amirhosein Zobeiri, Mahdi Dehghani, Mohammadali Mohammadkhani, Bardia Mohammadi, Omid Ghahroodi, Mahdieh Soleymani Baghshah, and Ehsaneddin Asgari. Ask in Any Modality: A Comprehensive Survey on Multimodal Retrieval-Augmented Generation, June 2025. URL <http://arxiv.org/abs/2502.08826>. arXiv:2502.08826 [cs].

[27] Yinghao Zhu, Changyu Ren, Shiyun Xie, Shukai Liu, Hangyuan Ji, Zixiang Wang, Tao Sun, Long He, Zhoujun Li, Xi Zhu, and Chengwei Pan. REALM: RAG-Driven Enhancement of Multimodal Electronic Health Records Analysis via Large Language Models, February 2024. URL <http://arxiv.org/abs/2402.07016>. arXiv:2402.07016 [cs].

[28] Peng Xia, Kangyu Zhu, Haoran Li, Tianze Wang, Weijia Shi, Sheng Wang, Linjun Zhang, James Zou, and Huaxiu Yao. MMed-RAG: Versatile Multimodal RAG System for Medical Vision Language Models, March 2025. URL <http://arxiv.org/abs/2410.13085>. arXiv:2410.13085 [cs].

[29] Chuwei Luo, Guozhi Tang, Qi Zheng, Cong Yao, Lianwen Jin, Chenliang Li, Yang Xue, and Luo Si. Bi-VLDoc: bidirectional vision-language modeling for visually-rich document understanding. *International Journal on Document Analysis and Recognition (IJDAR)*, 28(4): 669–680, December 2025. ISSN 1433-2833, 1433-2825. doi: 10.1007/s10032-025-00518-w. URL <https://link.springer.com/10.1007/s10032-025-00518-w>.

[30] Yiheng Chen, Lingyao Li, Zihui Ma, Qikai Hu, Yilun Zhu, Min Deng, and Runlong Yu. Empowering LLM Agents with Geospatial Awareness: Toward Grounded Reasoning for Wildfire Response, October 2025. URL <http://arxiv.org/abs/2510.12061>. arXiv:2510.12061 [cs].

[31] Kai Yin, Xiangjue Dong, Chengkai Liu, Lipai Huang, Yiming Xiao, Zhewei Liu, Ali Mostafavi, and James Caverlee. DisastIR: A Comprehensive Information Retrieval Benchmark for Disaster Management, September 2025. URL <http://arxiv.org/abs/2505.15856>. arXiv:2505.15856 [cs].

[32] National Geodetic Survey. Emergency response imagery, 2026. URL <https://storms.ngs.noaa.gov/>.

[33] Gemini Team. Gemini: A family of highly capable multimodal models. <https://deepmind.google/technologies/gemini/>, 2024.

[34] Wenhui Wang, Furu Wei, Li Dong, Hangbo Bao, Nan Yang, and Ming Zhou. Minilm: Deep self-attention distillation for task-agnostic compression of pre-trained transformers. 2020. URL <https://arxiv.org/abs/2002.10957>.

[35] Shitao Xiao, Zheng Liu, Peitian Zhang, Niklas Muennighoff, Defu Lian, and Jian-Yun Nie. C-pack: Packed resources for general chinese embeddings. In *Proceedings of the 47th International ACM SIGIR Conference on Research and Development in Information Retrieval, SIGIR '24*, page 641–649, New York, NY, USA, 2024. Association for Computing Machinery. ISBN 9798400704314. doi: 10.1145/3626772.3657878. URL <https://doi.org/10.1145/3626772.3657878>.

[36] Alec Radford, Jong Wook Kim, Chris Hallacy, Aditya Ramesh, Gabriel Goh, Sandhini Agarwal, Girish Sastry, Amanda Askell, Pamela Mishkin, Jack Clark, Gretchen Krueger, and Ilya Sutskever. Learning transferable visual models from natural language supervision, 2021. URL <https://arxiv.org/abs/2103.00020>.

[37] Abhimanyu Dubey et al. The Llama 3 Herd of Models, 2024. URL <https://arxiv.org/abs/2407.21783>.

[38] An Yang et al. Qwen2.5 Technical Report, 2025. URL <https://arxiv.org/abs/2412.15115>.

[39] OpenAI et al. GPT-4o System Card, 2024. URL <https://arxiv.org/abs/2410.21276>.

[40] FEMA. FEMA - Harvey flood depths grid. HydroShare, 2023. URL <https://doi.org/10.4211/hs.e8768f4cb4d5478a96d2b1cbd00d9e85>.

[41] Junwei Ma, Russell Blessing, Samuel Brody, and Ali Mostafavi. Non-locality and spillover effects of residential flood damage on community recovery: Insights from high-resolution flood claim and mobility data. *Sustainable Cities and Society*, 117:105947, 2024. ISSN 2210-6707. doi: <https://doi.org/10.1016/j.scs.2024.105947>. URL <https://www.sciencedirect.com/science/article/pii/S2210670724007716>.

Appendix A. Prompts

We provide the full prompts used in our experiments. The temporal context and semantic alignment instructions (highlighted in the system prompt) were critical for achieving best performance.

Appendix A.1. System Prompt (Multimodal)

The following system prompt is used for both Text+Caption and full Multimodal experiments:

You are an assistant estimating post-disaster impact for Harris County, TX during Hurricane Harvey. You will be provided with aerial imagery, text snippets, sensor data, and FEMA priors.

CRITICAL TEMPORAL CONTEXT:

- Hurricane Harvey PEAK FLOODING: August 27-28, 2017
- Aerial imagery captured: August 31, 2017 (3-4 days AFTER peak)
- By Aug 31, most floodwaters had RECEDED from streets
- Text reports (tweets/311 calls) are from DURING the event (real-time)

KEY INSIGHT:

If imagery shows "dry/clear" but text reports "flooded", the flooding DID happen - the water simply receded before the satellite captured the image. TRUST THE TEXT.

IMPORTANT: All provided text snippets (Tweets, 311 Calls) are pre-filtered and RELEVANT to the queried location/time.

DECISION RULES:

- For FLOOD EXTENT: PRIORITIZE text reports. Visual "no flooding" means water receded, NOT that it didn't flood.
- For STRUCTURAL DAMAGE: Visual IS reliable for persistent damage (debris, destroyed buildings). But if text reports damage and visual shows none, trust text (internal damage not visible).

SENSOR DATA INTERPRETATION (CRITICAL):

- Sensor data shows conditions DURING the query time window.
- Hurricane Harvey PEAK FLOODING was Aug 27-28, 2017.
- If query window is AFTER peak (e.g., Sept 1-10), sensor showing "0.0 inches" means water is RECEDED, NOT that flooding didn't happen.
- For flood extent, ALWAYS prioritize tweets/311 calls from DURING the event (Aug 27-28).
 - Sensor data from post-event periods (Sept+) should be interpreted as "storm has passed, water likely receding", not "no flooding occurred".
 - If tweets report flooding but sensor shows 0.0 during Sept, the flooding DID happen - water just receded by then.

DAMAGE SEVERITY INTERPRETATION:

- damage_severity_pct represents the AVERAGE damage per building in the ZIP (0-100%).

- This is NOT "overall severity" but rather: "What is the average % damage across all buildings?"
- If you see reports of "10 houses destroyed" in an area with ~100 buildings, estimate ~10% (10/100).
- If reports say "widespread damage" but don't specify counts, estimate based on proportion of reports mentioning damage vs total area.

CHAIN OF THOUGHT REASONING:

- In "reasoning", list every Tweet ID and 311 Call ID you see.
- Note any temporal discrepancy between text and imagery.
- For flood extent, base your estimate primarily on text evidence.

EXAMPLE:

Input Context:

- Images: [IMG_1] (shows clear roads - captured Aug 31)
- Tweets: [- [T123] (ZIP 77002, Aug 27) "Water entering my living room!"]

Correct Output Reasoning:

"Tweet T123 reports water in living room on Aug 27. Image IMG_1 from Aug 31 shows clear roads. This is expected - water receded by Aug 31. I estimate HIGH flood extent based on the tweet."

Respond with valid JSON matching the schema provided by the user.

Appendix A.2. Text-Only System Prompt

For the Text-Only baseline, we use a simplified prompt without visual references:

You are an assistant estimating post-disaster impact for Harris County, TX during Hurricane Harvey. You will be provided with text snippets (Tweets, 311 Calls), sensor data, and FEMA priors.

CRITICAL INSTRUCTION:

- You MUST analyze the provided Tweets and 311 Calls for on-the-ground reports.
- Cite specific Tweet IDs and Call IDs in your summary.
- Do NOT mention imagery or visual evidence, as none is provided.

SENSOR DATA INTERPRETATION (CRITICAL):

- Sensor data shows conditions DURING the query time window.
- Hurricane Harvey PEAK FLOODING was Aug 27-28, 2017.
- If query window is AFTER peak (e.g., Sept 1-10), sensor showing "0.0 inches" means water is RECEDED, NOT that flooding didn't happen.
- For flood extent, ALWAYS prioritize tweets/311 calls from DURING the event (Aug 27-28).
 - Sensor data from post-event periods (Sept+) should be interpreted as "storm has passed, water likely receding", not "no flooding occurred".
 - If tweets report flooding but sensor shows 0.0 during Sept, the flooding DID happen - water just receded by then.

```

## DAMAGE SEVERITY INTERPRETATION:
- damage_severity_pct represents the AVERAGE damage per building
  in the ZIP (0-100%).
- This is NOT "overall severity" but rather: "What is the average %
  damage across all buildings?"
- If you see reports of "10 houses destroyed" in an area with ~100
  buildings, estimate ~10% (10/100).
- If reports say "widespread damage" but don't specify counts, estimate
  based on proportion of reports mentioning damage vs total area.
- Base estimates on counts of damaged buildings mentioned in
  reports, not just severity of individual cases.

```

Respond with valid JSON matching the schema provided by the user.

Appendix A.3. User Prompt Template

Each query includes temporal warnings for captions and sensor data, FEMA prior knowledge, and the full output schema:

```

ZIP: {zip_code}
Time window: {start} to {end}
Imagery IDs: {imagery_tile_ids}

    ### Sensor Data (Precipitation):
    Warning: This sensor data is from {start_date} (query time window).
    If this date is AFTER Aug 28 (peak flooding), sensor showing "0.0"
    means storm passed/water receding, NOT that flooding didn't happen.
    Prioritize tweets/311 calls from Aug 27-28 for flood extent.
{sensor_table}

    ### FEMA Prior Knowledge (Historical Context):
{kb_summary}

    ### Tweets (Relevant to ZIP {zip_code}) - REAL-TIME REPORTS:
- [{tweet_id}] (ZIP {zip_code}) {tweet_text}
...
    ...

    ### 311 Calls (Relevant to ZIP {zip_code}) - REAL-TIME REPORTS:
- [{call_id}] (ZIP {zip_code}) {call_description}
...
    ...

    ### Image Captions (TEMPORAL WARNING):
**These captions describe imagery from Aug 31, 2017 - AFTER peak flooding
(Aug 27-28).**
**By Aug 31, floodwaters had RECEDED. "No flooding visible" does NOT
mean flooding didn't occur!**

- For FLOOD EXTENT: IGNORE these captions. Trust tweets/311 calls instead.
- For STRUCTURAL DAMAGE: These captions ARE useful (damage is persistent).

```

```

{caption_list}

Respond with JSON matching schema:
{
  "reasoning": str, // Your analysis of the evidence
  "zip": str,
  "time_window": {"start": str, "end": str},
  "estimates": {
    "flood_extent_pct": float, // HAZARD: % of ZIP area covered by
                                // floodwater (0-100). Base on Imagery +
                                // Water Reports.
    "damage_severity_pct": float, // CONSEQUENCE: Average structural
                                // damage per building (0-100).
                                // This represents the MEAN damage
                                // across all buildings in the ZIP.
    "roads_impacted": list[str],
    "confidence": float // 0-1
  },
  "evidence_refs": {
    "imagery_tile_ids": list[str],
    "tweet_ids": list[str],
    "call_311_ids": list[str],
    "sensor_ids": list[str],
    "kb_refs": list[str]
  },
  "natural_language_summary": str
}

```

Appendix A.4. Query Parsing Prompt

For the natural language chat interface, we use a query parsing prompt to extract structured parameters from user requests:

You are a query parser for a disaster impact assessment system. Your goal is to extract structured parameters from a natural language user request. The user is asking about Hurricane Harvey impact in a specific location and time.

Extract the following fields:

- zip: The 5-digit ZIP code (e.g., "77096"). If missing, return null.
- start: The start date in YYYY-MM-DD format.
- end: The end date in YYYY-MM-DD format.

If only one date is mentioned, use it for both start and end.

If no year is mentioned but "Harvey" is implied, assume 2017.

If no date is mentioned, return null for dates.

Respond with valid JSON only.

The user message is then formatted as:

```
User Message: "{message}"  
  
Respond with JSON matching schema:  
{  
  "zip": str | null,  
  "start": str | null,  
  "end": str | null  
}
```

Appendix B. Tweet Filtering Keywords

We implemented a keyword-based filtering pipeline to improve the signal-to-noise ratio of the ~24 million raw tweets. A tweet is included if it contains at least one allow keyword and no block keywords.

Appendix B.1. Allow List

Keywords that indicate disaster-relevant content:

| | | | |
|---------|----------|------------|-----------|
| flood | flooding | flooded | hurricane |
| storm | rain | underwater | rescue |
| trapped | stuck | help | emergency |
| 911 | evacuate | damage | collapsed |
| power | outage | road | bridge |
| bayou | creek | | |

Appendix B.2. Block List

During initial corpus exploration, we observed that many tweets containing disaster-related terms (e.g., Harvey, Houston) were unrelated to the hurricane. Common sources of noise included: (1) music promotion and streaming service spam using trending hashtags; (2) political commentary co-opting the disaster for unrelated messaging; (3) commercial advertisements and promotional giveaways; and (4) sports and entertainment discussions. The block list was developed iteratively by examining false positives in the filtered corpus.

Keywords that indicate irrelevant content:

| | | | |
|----------|-----------|----------|----------|
| spotify | music | song | album |
| lyrics | vote | election | trump |
| biden | president | giveaway | contest |
| win | sale | shirt | merch |
| game | nfl | nba | football |
| baseball | love | heart | tears |

This filtering reduced the corpus from ~24 million to 458,453 tweets (~1.9% acceptance rate).

Appendix C. Successful Examples

We present two success cases demonstrating accurate flood extent prediction when evidence is convergent and correctly interpreted.

Success Case 1: Precise Regional Inference (ZIP 77447). Ground Truth: 30.5% | Prediction: 25.0% | Abs. Error: 5.5 pp

Retrieved Evidence: Tweets (20): “Houston braces for impact from Hurricane Harvey” (901377628594196481); “Texas Flood Damage From Harvey May Match Katrina” (901917030970003457); “Hurricane Harvey destroyed a lot” (903081533124247553). Sensor: 0.0 inches (Sept 10), correctly interpreted as “water is receding.” 311 Calls: None retrieved. Imagery: Visual analysis unavailable.

Model Reasoning: “No specific on-the-ground reports directly mention flooding within ZIP 77447. However, tweets indicate widespread regional impact from Hurricane Harvey across Houston. Given that 77447 is within Harris County, it is highly probable it experienced some degree of flooding consistent with regional impact. The sensor data showing 0.0 inches indicates water had receded by the post-event date and does not contradict flooding during the query window.”

Why It Worked: The model correctly calibrated its estimate based on regional context without over-extrapolating. The absence of specific local reports led to a moderate conservative estimate (25%) rather than extreme values, which aligned closely with ground truth.

Success Case 2: Intelligent Inference (ZIP 77067). Ground Truth: 59.5% | Prediction: 60.0% | Abs. Error: 0.5 pp

Retrieved Evidence: Tweets (20): “Hurricane Harvey Relief @ GHIC 200 W Greens Rd Houston Texas 77067” (903033982874517505); “Harvey unleashes historic flooding in Houston area” (901826476210876417); “Hurricane Harvey destroyed a lot” (903081533124247553). Sensor: 0.0 inches (Sept 10), correctly interpreted as post-event recession. 311 Calls: None retrieved. Imagery: Visual analysis unavailable.

Model Reasoning: “Multiple tweets mention a ‘Hurricane Harvey Relief’ @ 200 W Greens Rd Houston Texas 77067 dated August 30, 2017. The establishment of a relief center directly within the ZIP code strongly indicates that the area experienced significant impact from the hurricane, necessitating aid and support. General tweets describing Harvey as a ‘historic flooding’ event further contextualize the severe conditions. The presence of a relief center suggests a notable portion of the area was affected by flooding.”

Why It Worked: The model successfully identified a critical semantic cue, the presence of a relief center, to infer high impact even in the absence of direct ‘flooding’ reports for that specific ZIP. This demonstrated the value of RAG in bringing in diverse evidence types.